

DOI: 10.63527/1607-8829-2025-2-36-48

I.V. Horichok¹ (<https://orcid.org/0000-0001-9748-3288>),
M.O. Halushchak² (<https://orcid.org/0009-0000-3693-4903>),
O.H. Kulyk¹ (<https://orcid.org/0009-0001-2499-6813>)
T.S. Potiatynnyk¹ (<https://orcid.org/0009-0004-7067-7639>)

¹Vasyl Stefanyk Precarpathian National University,
 Ivano-Frankivsk, 76018, Ukraine;

²Ivano-Frankivsk National Technical University
 of Oil and Gas, Ivano-Frankivsk, 76000, Ukraine

Corresponding author: I.V. Horichok, e-mail: Ihor.Horichok@pnu.edu.ua

Calculation of Charge Carrier Mobility in PbTe Based on Empirical Thermoelectric Parameters

The paper presents a comparative analysis of the charge carrier mobility in PbTe calculated using expressions derived from the Drude-Sommerfeld model and the model of a nondegenerate semiconductor with parabolic zones. The mobilities were calculated as functions of the experimentally determined Seebeck coefficient and specific electrical conductivity. The results are compared with the corresponding data obtained in the relaxation time approximation.

Keywords: mobility, Seebeck coefficient, specific electrical conductivity, effective mass.

Introduction

Mobility is an important parameter of the electronic subsystem used to assess the thermoelectric quality of materials [1–3]:

$$B = \left(\frac{k_0}{e_0} \right)^2 e_0 N_{C,V} \frac{u}{k_{lat}} T. \quad (1)$$

Here, $N_{C,V}$ is the density of states in conduction band (N_C) or valence band (N_V). The thermoelectric figure of merit ZT is related to B [3]:

$$ZT = \frac{A(\mu)}{B + C(\mu)}, \quad (2)$$

Citation: I.V. Horichok, M.O. Halushchak, O.H. Kulyk, T.S. Potiatynnyk (2025). Calculation of Charge Carrier Mobility in PbTe Based on Empirical Thermoelectric Parameters. *Journal of Thermoelectricity*, (2), 36–48. <https://doi.org/10.63527/1607-8829-2025-2-36-48>

where $A(\mu)$ and $B(\mu)$ are functions that depend only on the chemical potential and are combinations of Fermi integrals with different indices. And the thermoelectric figure of merit, as is known, is an integral characteristic of material and allows one to determine the efficiency of thermal into electric energy conversion, in particular, according to the dependence [4]:

$$Z = \frac{T_h - T_c}{T_h} \frac{\sqrt{ZT + 1} - 1}{\sqrt{ZT + 1} + T_h/T_c}. \quad (3)$$

Thus, the parameter B reflects a combination of the main parameters of the material, including the mobility of charge carriers. The numerical value of this quantity will determine the fundamental possibility of the material's suitability for practical use in thermoelectric converters. At the same time, the numerical values of the terms $A(\mu)$ and $B(\mu)$ can be relatively easily optimized, for example, by doping, to achieve the maximum value of ZT at a given B .

The main experimental method for measuring the carrier mobility u is the study of the Hall effect. However, conducting such studies is often a relatively difficult task, in particular at high temperatures. A separate difficulty also arises when the concentrations of the majority and minority carriers are of the same order of magnitude, which is also often the case at high temperatures. The difficulty in this case lies in separating the contribution of the electron and hole subsystems. Therefore, in [5] a relatively simple method of calculating u was presented. The mobility expression presented by the authors was obtained in the approximate Drude-Sommerfeld model of free electrons and involves the use of experimentally measured values of the Seebeck coefficient and specific electrical conductivity for calculations:

$$u_w = \frac{3h^3 \sigma}{8\pi e_0 (2m_0 k_0 T)^{3/2}} \left[\frac{\exp\left(\frac{|S|}{k_0/e_0} - 2\right)}{1 + \exp\left(-5\left(\frac{|S|}{k_0/e_0} - 1\right)\right)} + \frac{\frac{3|S|}{\pi^2 k_0/e_0}}{1 + \exp\left(-5\left(\frac{|S|}{k_0/e_0} - 1\right)\right)} \right] \quad (4)$$

Here, m_0 is the mass of a free electron. According to [5], the thus determined mobility u_w (w – weighted) is related to the Hall mobility u_H through the effective mass of the density of states:

$$u_w = u_H \left(\frac{m_{d,0}^*}{m_0} \right)^{3/2} \quad (5)$$

That is, if in (4) instead of m_0 we immediately substitute $m_{d,0}^*$, we obtain the Hall mobility. On the other hand, if $S(T)$, $\sigma(T)$ and the Hall mobility $u_H(T)$ are measured, we can obtain the temperature dependence of the effective mass of the density of states $m_{d,0}^*(T)$, which was done in particular in [6] and [7].

In [6], the thermoelectric properties of SnS doped with sodium and selenium were investigated. Based on the measurements of the Seebeck coefficient and specific electrical conductivity, the authors calculated the mobility u_w . Additionally, the Hall mobility was measured, which allowed determining the temperature dependence of the effective mass of the density of states using expression (5). The obtained dependence was characterized by non-monotonic behavior, with a maximum around 750 K. The authors made the assumption that it is at this temperature that the mutual arrangement of the three valence subbands is closest and this is the reason for the growth of the effective mass of the density of states. Using the obtained values of the effective mass, the authors calculated the thermoelectric quality of the material, through which, in turn, they determined the thermoelectric figure of merit ZT . The results of such a calculation are in good agreement with the results of the calculation of ZT based on the measured S , σ , k .

In [7], the calculation of the mobility u_w and its comparison with the Hall mobility were also used to estimate the change in the effective masses of the density of states with an increase in the amount of introduced impurity.

Thus, this approach can be useful not only for calculating mobilities and further assessing the thermoelectric quality of materials, but also for determining the effective mass of the density of states, if such a parameter is unknown. However, it is worth bearing in mind the approximation of the model within which expression (4) is obtained. The Drude-Sommerfeld model at one time turned out to be very productive for explaining the properties of metals. Degenerate superconductors often exhibit properties similar to metals. For example, the temperature dependence of the specific electrical conductivity σ decreases with a rise in temperature, as in metals. Also, in the case of strong degeneracy, the expressions for the kinetic parameters may not depend explicitly on the scattering mechanism [8]. The corresponding equations, like equation (4), will not contain the parameter r , which characterizes a specific scattering mechanism ($r = 0$ for scattering on the deformation potential of acoustic (DA) and optical phonons (DO), $r = 1$ for scattering on the polarization potential of optical phonons (PO), $r = 2$ for scattering on an ionized impurity (ID))[8].

However, it is known that good thermoelectric materials are weakly degenerate semiconductors. Therefore, the model valid for strong degeneracy may lead to an error in the estimation of u . In this work, we compared the mobilities obtained by formula (4) and by sequential calculation in the relaxation time approximation. We also analyzed the possibility of using another expression for the mobility u as a function of σ and S , obtained for non-degenerate semiconductors with parabolic zones. The results were compared with experimental data. Model calculations were performed for iodine-doped lead telluride PbTe:I, since doping with I does not form localized energy levels that can cause additional scattering mechanisms at certain Fermi energy values. We also used the experimental dependences $S(T)$, $\sigma(T)$ from [9], where the hot pressing method was used to obtain experimental samples, which also excludes the participation of grain boundaries in scattering processes. In addition, for PbTe there is sufficient information on the effective masses [9], which, in general, makes this material a good model object.

Calculation method and results

The method of calculating u in the relaxation time approximation is presented, in particular, in [3, 8, 10]. The mobility in these works is defined as:

$$u = e \frac{\tau_0(T)}{m_{n,0}} \cdot \frac{I_{r+1,2}^0(\eta, \beta)}{I_{3/2,0}^0(\eta, \beta)}. \quad (6)$$

Here, $m_{n,0}$ is the effective mass at the bottom of the zone, τ_0 is the carrier relaxation time, $I_{n,k}^m(\eta, \beta)$ is the Fermi integral. According to [8]:

$$I_{n,k}^m(\eta, \beta) = \int_0^\infty \left(-\frac{\partial f_0}{\partial x} \right) \frac{x^m (x + \beta x^2)^n dx}{(1 + 2\beta x)^k}. \quad (7)$$

Here, $x = E/k_0T$ is the reduced energy, $\eta = \mu/k_0T$ is the reduced Fermi energy, $\beta = k_0T/E_g$ is the nonparabolicity index, $f_0 = 1/(1 + e^{x-\eta})$ is the Fermi function. The Fermi energy was determined by fitting the calculated values of $\sigma(T)$ to the experimental ones by varying μ .

The specific electrical conductivity was determined according to the dependence

$$\sigma = une_0, \quad (8)$$

In which the carrier concentration n was defined as:

$$n = \frac{(2m_{d,0}^*kT)^{\frac{3}{2}}}{3\pi^2\hbar^3} I_{3/2,0}^0(\eta, \beta), \quad (9)$$

The relaxation time of carriers in the case of scattering on the deformation potential of acoustic phonons:

$$\tau_{0r}(T) = \frac{2\pi\hbar^4\rho v_0^2}{(2m_{n,0}k_0T)^{\frac{3}{2}} E_1^2}, \quad (10)$$

where $\rho = 8.24 \text{ g/cm}^3$ [10], $E_1 = 15 \text{ eV}$ [10], $v_0 = 1.92 \text{ km/s}$ [11]).

When scattering on the deformation potential of optical phonons (for $k_0T \gg \hbar\omega_0$):

$$\tau_{0r}(T) = \frac{2}{\pi} \left(\frac{\hbar\omega_0}{E_0} \right)^2 \frac{\hbar^2 a^2 \rho}{(2m_{n,0}k_0T)^{\frac{3}{2}}}, \quad (11)$$

where $\hbar\omega_0 = k\theta$ ($\theta = 157.8 \text{ K}$ [3]), $a = 6.461 \text{ \AA}$ [10], $E_0 = 26 \text{ eV}$ [10].

When scattering on the polarization potential of optical phonons (for $k_0T \gg \hbar\omega_0$):

$$\tau_{0r}(T) = \frac{\hbar^2}{e^2 \sqrt{2m_n k_0 T} \left(\frac{1}{\chi_\infty} - \frac{1}{\chi_0} \right)}, \quad (12)$$

where $\chi_\infty = 32.6$ [10]; $\chi_0 = 400$ [10].

The calculation took into account corrections for the Bloch form of the wave functions and shielding. According to [8], this correction for acoustic phonons is defined as:

$$F_{ak}(k) = 1 - \frac{10}{3}L + \left[\frac{191}{60} + \frac{11}{60} \left(\frac{v_L}{v_T} \right)^2 \right] L^2, \quad (13)$$

where v_L and v_T are the longitudinal and transverse components of the speed of sound. When scattering on the deformation potential of optical phonons [8]:

$$F_{KP} = 1 - \frac{8}{3}L + \frac{13}{6}L^2 \quad (14)$$

When scattering on the polarization potential of optical phonons [8]:

$$F'_{PO} = 1 - \frac{2}{\xi} \ln(1 + \xi) + \frac{1}{1 + \xi} - \frac{1}{2} (4L - L^2) B + L^2 C \quad (15)$$

$\xi = (2kr_0)^2$, where k is wave number, r_0 is shielding radius.

In the above formulae: $L = \frac{E}{E_g + 2E}$, $B = 1 - \frac{4}{\xi} - \frac{2}{\xi(1 + \xi)} + \frac{6}{\xi^2} \ln(1 + \xi)$,

$C = 1 - \frac{3}{\xi} + \frac{9}{\xi^2} + \frac{3}{\xi^2(1 + \xi)} - \frac{12}{\xi^3} \ln(1 + \xi)$. The shielding radius when calculating ξ was

determined as [8] $r_0^2 = \frac{\chi_0 k_0 T}{6\pi e^2 n} \cdot \frac{I_{3/2,0}^0(\eta, \beta)}{I_{1/2,-1}^0(\eta, \beta)}$. The wave number $k = \sqrt{\frac{2m_{n,0}}{\hbar^2} \bar{E} \left(1 + \frac{\bar{E}}{E_g} \right)}$, where

$\bar{E} = \frac{1}{n} \int_0^\infty E \cdot g(E) \cdot f_0(E, \mu) dE$, and $n = \int_0^\infty g(E) \cdot f_0(E, \mu) dE$. The density of states

$g(E) = \frac{(2m_{d,0})^{\frac{3}{2}}}{2\pi^2 \hbar^3} E^{\frac{1}{2}} \left(1 + \frac{E}{E_g} \right)^{\frac{1}{2}} \left(1 + \frac{2E}{E_g} \right)$. The correction was taken into account by dividing the

corresponding values of τ_0 by the correction.

Fig. 1 shows the mobilities calculated in this way as a function of the carrier concentration for impurity-free PbTe at 300 K and compared with experimental data [10]. It can be seen that, firstly, the model describes the experiment well in the concentration range $\geq 10^{19} \text{ cm}^{-3}$, and, secondly, the mobility in this range is determined to an approximately equal extent by DA, DO and PO.

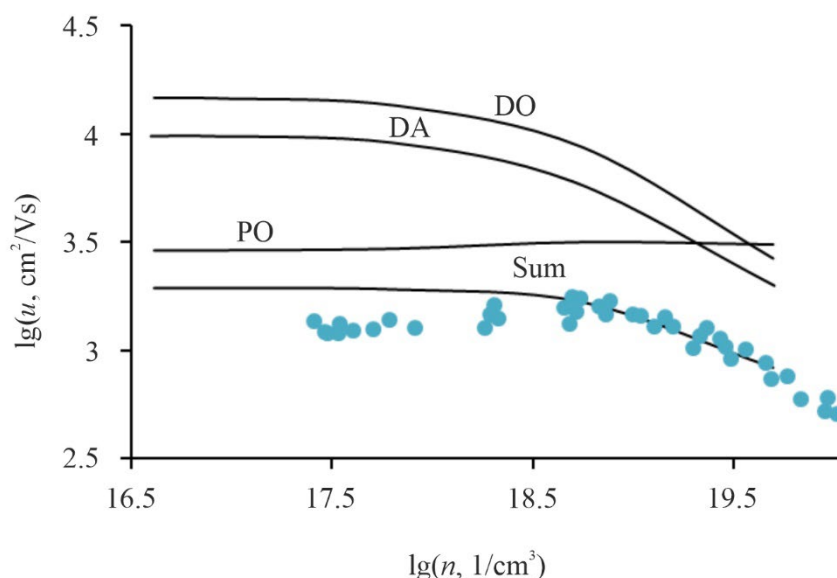


Fig. 1. Dependence of electron mobility in PbTe on their concentration at 300 K. Sum is mobility obtained with regard to three scattering mechanisms (DA+DO+PO); DA is partial contribution due to scattering on the deformation potential of acoustic phonons; DO is partial contribution due to scattering on the deformation potential of optical phonons; PO is partial contribution due to scattering on the polarization potential of optical phonons. Dots are experimental data [10]

Fig. 2 shows the calculation of the temperature dependences of mobilities for iodine-doped lead telluride PbTe:I in the relaxation time approximation and using the experimental dependences $S(T)$ and $\sigma(T)$ and expression (4). The calculation was performed for the effective mass $m_{d,0}^* = 0.142 \cdot (T/120)^{0.4} \cdot m_0$, which is known for PbTe [12], and also using the one determined in [9] $m_{d,0}^* = 0.25 \cdot (T/300)^{0.5} \cdot m_0$.

We see that when using the relaxation time method, the calculated and experimental values correlate very well near room temperatures, and at higher temperatures the correlation deteriorates. Formula (4) works well only in the high T region, while in the T_{room} region the calculated mobility and experimental values differ by a factor of three.

Given the approximation of formula (4), the obtained result is relatively satisfactory, especially if we take into account that the only parameter required for the calculation is the effective mass of the density of states $m_{d,0}^*$. In the case of the relaxation time, a much larger number of parameters is required, in particular, the electron-phonon interaction constants, the determination of which is a difficult task.

To establish the reasons for the observed discrepancies, in particular due to the influence of the self-carriers n_i on the result of the calculation of $u_w(T)$, we calculated their concentrations in PbTe and the total concentration n for the studied material PbTe:I. The Fermi energy μ and the concentration n were obtained when calculating u in the relaxation time approximation. It is important to note that the calculated value of n at 300 K is $3.1 \cdot 10^{19} \text{ cm}^{-3}$, which is in very good agreement with the experimental $2.9 \cdot 10^{19} \text{ cm}^{-3}$ [9].

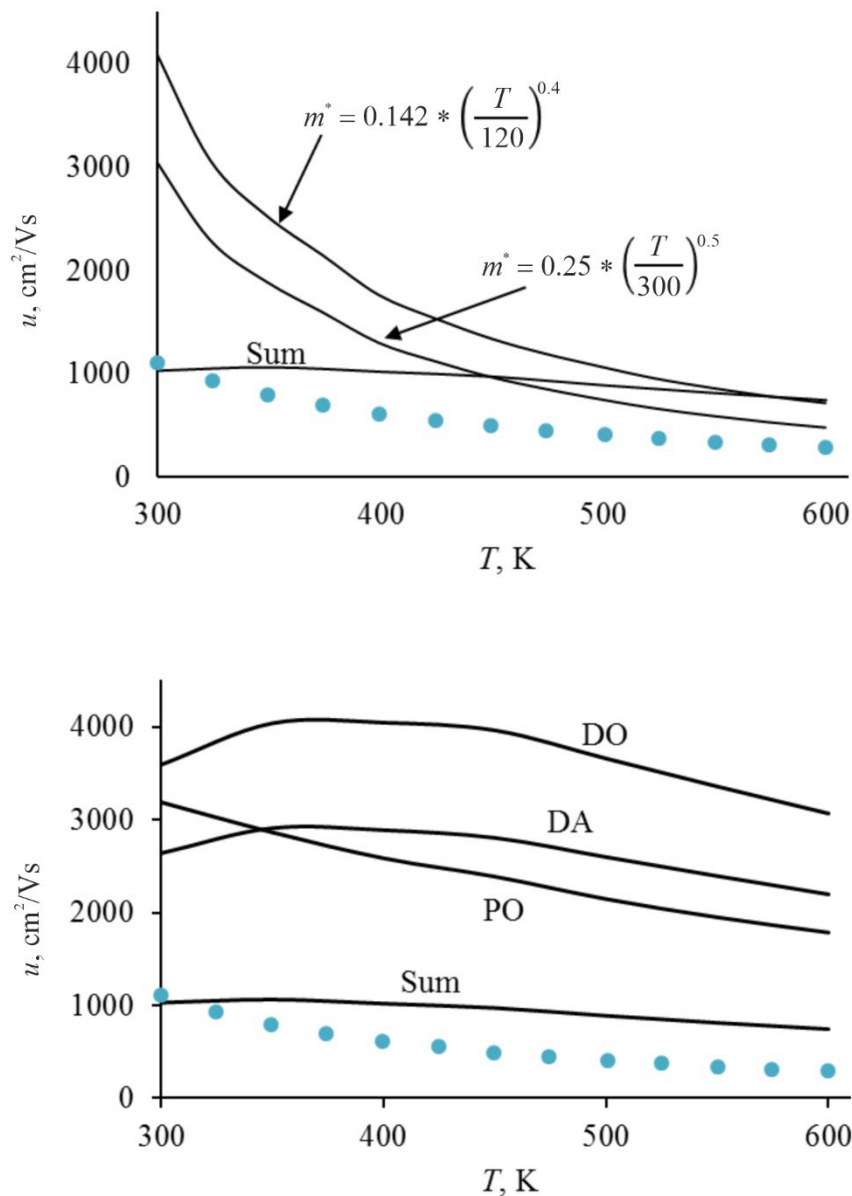


Fig. 2. a – the dependence of the electron mobility in PbTe:I on temperature was obtained in the relaxation time approximation (Sum) taking into account three scattering mechanisms (DA+DO+PO), and by formula (4) at two different values of the effective mass of the density of states; b – partial contributions of each of the scattering mechanisms were obtained when calculating the mobility in PbTe:I in the relaxation time approximation (the designation of the mechanisms is similar to Fig. 1). Experimental data – [9]

The calculation of n_i was performed according to the dependence $n_i = \sqrt{N_C N_V} \exp(-E_g/2k_0T)$. In this case, the concentration for $E_g = E_C - E_{V,l}$ and for $E_g = E_C - E_{V,h}$ was calculated separately. And n_i was determined as the sum of the concentrations obtained in these two calculations. The non-parabolicity of the zones (the dependence $m^*(\mu)$) was not taken into account, since μ for the intrinsic semiconductor should be near the middle of the band gap. The nonparabolicity of the zones (the dependence $m^*(\mu)$)

was not taken into account, since μ for the intrinsic semiconductor should be near the middle of the band gap. The results of such a calculation are fully consistent with the data [13]. The band gap width between the conduction band and the valence band of the light holes was taken equal to $E_C - E_{V,l} = 0.19 - 4 \cdot 10^{-4}T$, eV, and between the conduction band and the valence band of heavy holes $E_C - E_{V,h} = 0.38$ eV [3].

As can be seen from Fig. (3), n is at least an order of magnitude greater than the concentration of intrinsic carriers n_i . And at room T , this difference is about three orders of magnitude. Consequently, intrinsic carriers are not the cause of the discrepancy between u_w and u_{exp} , especially at T_{room} . However, it can be assumed that taking them into account (n_i) could improve the correlation with experimental data for the relaxation time method at high T .

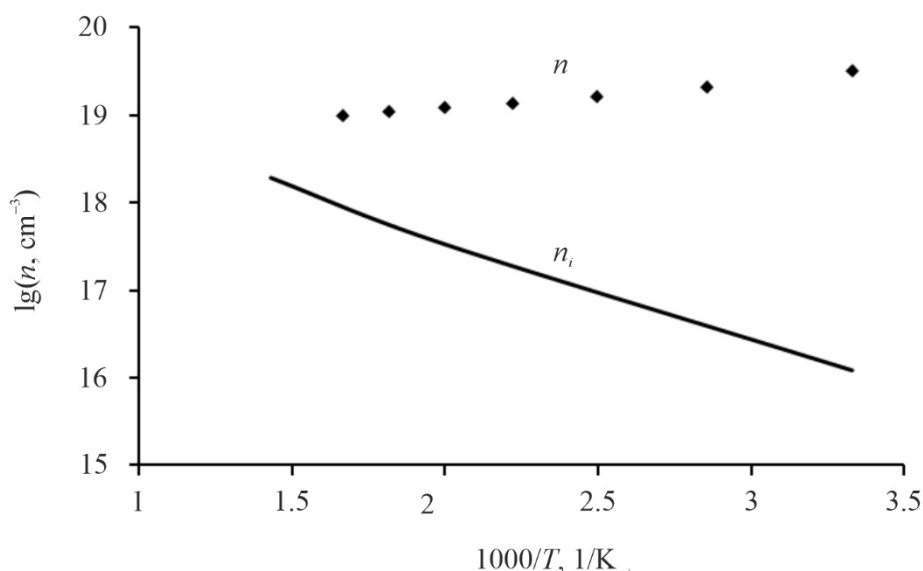


Fig. 3. Calculated temperature dependence of carrier concentration in PbTe:I (n), and the intrinsic carrier concentration in PbTe (n_i)

Fig. 4 shows the dependence of the chemical potential on the temperature obtained when calculating the specific electrical conductivity and mobility in the relaxation time approximation. As we can see, at 300 K μ is deep in the conduction band: deeper than $5 kT$. At 600 K – about $2 kT$. That is, at 300 K the material is closer to strong degeneracy ($10 kT$) than at 600 K. One could assume that with stronger degeneracy the Drude-Sommerfeld model, and hence formula (4), should give values closer to the experimental ones. However, the situation is the opposite.

In the region of weak semiconductor degeneracy ($-4 \cdot kT \leq \mu \leq 10 \cdot kT$) it is difficult to obtain simple analytical expressions, such as (4), for the kinetic parameters. But it would be interesting to evaluate the differences between the results of using formula (4), valid for the case of carrier degeneracy, and the formula obtained in the approximation of a non-degenerate semiconductor. It can be obtained using the dependence for the Seebeck coefficient known for this case:

$$S = \frac{k_0}{e_0} \left(r + 2 - \ln \left(\frac{n}{N_C} \right) \right), \quad (16)$$

where $N_C = 2 \left(\frac{2\pi m_{d,0}^* k_0 T}{h^2} \right)^{3/2}$ – the density of states in conduction band. Whence we obtain:

$$n = N_C \cdot \exp \left(r + 2 - \frac{S}{k_0/e_0} \right). \quad (17)$$

Since $u = \sigma / n e_0$, then

$$u = \frac{\sigma}{N_C e_0} \cdot \exp \left(\frac{S}{k_0/e_0} - (r + 2) \right). \quad (18)$$

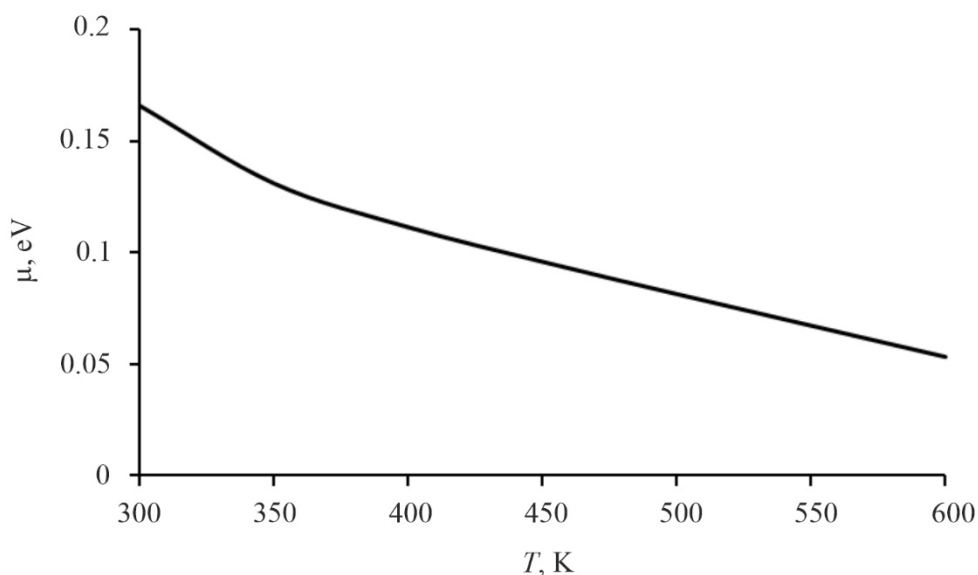


Fig. 4. The temperature dependence of the electron Fermi energy μ calculated in the relaxation time approximation while simultaneously taking into account three carrier scattering mechanisms (DA+DO+PO).

So, in this case, unlike expression (4), in addition to $m_{d,0}^*$ it is necessary to know the scattering parameter r . With a known dependence $\sigma_{exp}(T)$ it can be determined by the slope of the dependence $\ln(\sigma) - \ln(T)$ (Fig. 5). The parameter r itself, as noted above, can take on three values (0, 1, 2). These three values of r correspond to three different values of the tangent of the angle of inclination of the dependence $\sigma(T)$ in logarithmic coordinates [8]. In the case of n -PbTe, it is additionally necessary to take into account the temperature dependence of the effective mass $m^* = f(T)$. Then, when scattering electrons on the deformation potential of acoustic and optical phonons, the tangent of the angle will be -2.5 , and when scattering on the

polarization potential of optical phonons – – 1.1. For most A^4B^6 compounds, it is believed that scattering on the deformation potential of acoustic phonons (DA) almost always prevails over other mechanisms. However, as can be seen from Fig. 5, the slope of the experimental dependence is -2.1 . Based on this, it can be assumed that DA will not be the only determining scattering mechanism, as is obtained in the relaxation time approximation (Fig. 2, *b*).

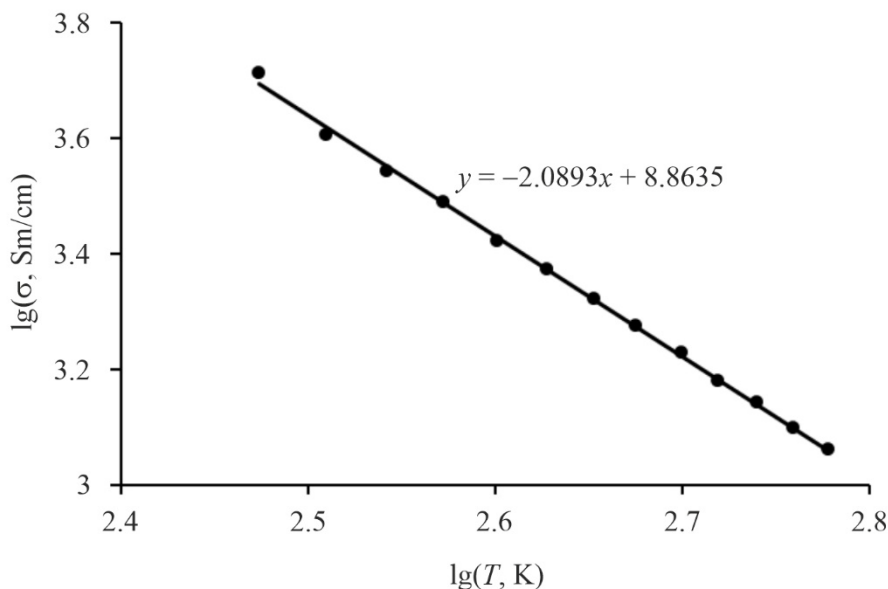


Fig. 5. Linear approximation of the temperature dependence of specific electrical conductivity in logarithmic coordinates for PbTe crystals: 1. Dots are experimental data [9], straight line is the approximation dependence

Fig. 6 shows the calculation of $u(T)$ using the obtained expression (18) for two values of r : 0 and 1. Also used $m_{d,0}^* = 0.142 \cdot (T / 120)^{0.4} \cdot m_0$ from [12] and $m_{d,0}^* = 0.25 \cdot (T / 300)^{0.5} \cdot m_0$ from [9]. We see that in the case of $r = 1$ and the effective mass from [12] at temperatures up to 450 K, the calculated mobility describes the experimental data well. But at higher temperatures, the model of dominance of scattering by optical phonons, for which $r = 1$, is more correct. Thus, for a quantitatively correct interpretation of the experimental data, it is necessary to take into account two scattering mechanisms simultaneously.

In [9], the authors calculated the effective mass of conduction electrons by fitting the calculated curve $u(T)$ to the experimental $u_H(T)$. In doing so, the authors used the model of dominance of scattering on the deformation potential of acoustic phonons. Fig. 7 shows the dependence obtained in [9] in comparison with the one known for lead telluride $m_{d,0}^* = 0.142 \cdot (T / 120)^{0.4} \cdot m_0$. Also in the figure, the dots represent the effective mass calculated by us according to the method described in the review. That is, first u_w was calculated according to (4), and then $m_{d,0}^*$, according to (5). We see that the difference from the other two dependences is significant.

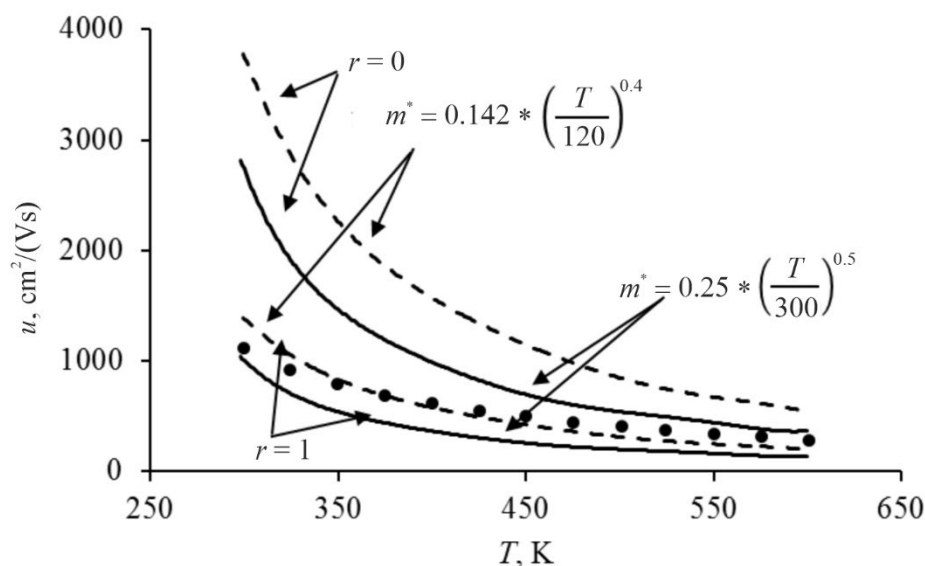


Fig. 6. The temperature dependences of the mobility obtained using expression (18) and experimental values from [9]

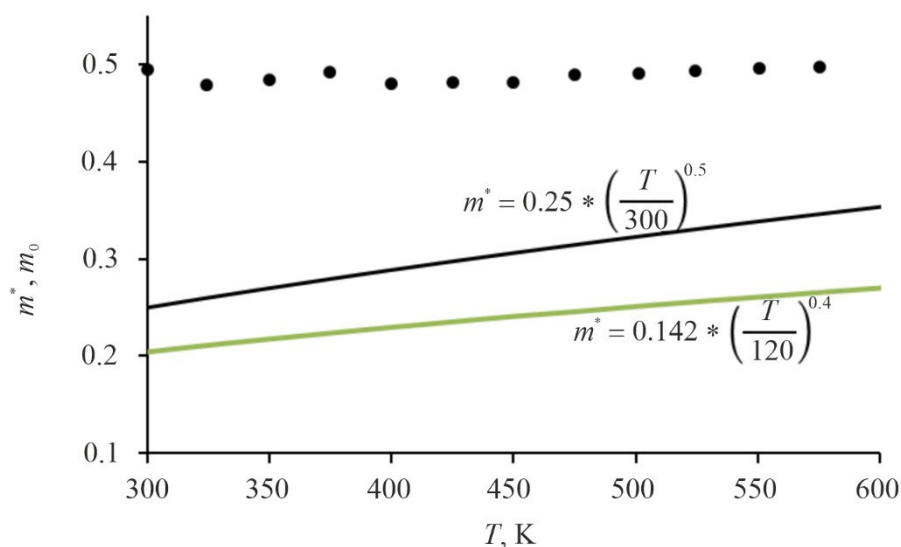


Fig. 7. Dependence of the effective mass of the density of states on temperature according to data from [12] ($m_{d,0}^* = 0.142 \cdot (T/120)^{0.4} \cdot m_0$), [9] ($m_{d,0}^* = 0.25 \cdot (T/300)^{0.5} \cdot m_0$) and obtained on the basis of calculations using formulae (4) and (5) (dots)

Conclusions

Calculation of the charge carrier mobility u as a function of the Seebeck coefficient S and the specific electrical conductivity σ in the Drude-Sommerfeld approximation makes it possible to obtain satisfactory numerical values in the temperature range $T > 450$ K. However, at room temperatures, the difference between the values of u calculated in this way and the experimental

ones is $\approx 300\%$. Using the expression obtained in the approximation of a nondegenerate semiconductor for calculating u makes it possible to obtain numerical values that, with the correct choice of the scattering parameter r , agree much better with the experiment.

Using the method of calculating the effective mass of the density of states through the calculation of the mobility u_w for PbTe:I leads to values that differ significantly from the known literature data.

Authors' information

- I.V. Horichok – Professor at the Department of Physics and Chemistry of Solids State.
- M.O. Halushchak – Professor at the Department of Physical and Mathematical Sciences.
- O.H. Kulyk – 1 category specialist at the Aspirants and Doctorate Department.
- T.S. Potiatynnyk – Student.

References

1. Joffe A.F., Stil'bans L.S. (1959) Physical problems of thermoelectricity. *Reports Prog. Phys.* 22 (1), 167–203. <https://doi.org/10.1088/0034-4885/22/1/306>.
2. Gelbstein Y., Davidow J. (2014). Highly efficient functional $\text{Ge}_x\text{Pb}_{1-x}\text{Te}$ based thermoelectric alloys. *Phys. Chem. Chem. Phys.*, 16, 20120-20126. DOI: 10.1039/C4CP02399D.
3. Khshanovska O., Parashchuk T., Horichok I. (2023). Estimating the upper limit of the thermoelectric figure of merit in n - and p -type PbTe. *Materials Science in Semiconductor Processing*, 160, 107428 (13p). <https://doi.org/10.1016/j.mssp.2023.107428>.
4. Ni J.E. (2012). Powder processing and mechanical properties of $\text{Ag}_{0.86}\text{Pb}_{19}\text{SbTe}_{20}$ (LAST) and $\text{Pb}_{0.95}\text{Sn}_{0.05}\text{Te}$ - PbS 8% (PbTe-PbS) thermoelectric materials. *A dissertation doctorate of philosophy Materials Science Engineering*. Michigan State University. P.300.
5. Snyder G.J., Snyder A.H., Wood M., Gurunathan R., Snyder B.H., Niu Ch. (2020). Weighted mobility. *Adv. Mater.*, 32, 2001537. DOI: 10.1002/adma.202001537.
6. He W., Qin B., Zhao L.-D. (2020). Predicting the potential performance in p -type SnS crystals via utilizing the weighted mobility and quality factor. *Chin. Phys. Lett.*, 37(8), 087104. DOI: 10.1088/0256-307X/37/8/087104.
7. Qin B., He W., Zhao L.-D. (2020). Estimation of the potential performance in p -type SnSe crystals through evaluating weighted mobility and effective mass. *Journal of Materiomics*, 6, 671e676. <https://doi.org/10.1016/j.jmat.2020.06.003>
8. Askerov B.M. (1994). *Electron transport phenomena in semiconductors*. <https://doi.org/10.1142/1926>.
9. Pei Y., LaLonde A. D., Wang, H. and Snyder G.J. (2012). Low effective mass leading to high thermoelectric performance. *Energy Environ. Sci.*, 5, 7963. DOI: 10.1039/c2ee21536e.
10. Zayachuk D.M. (1997). The dominant mechanisms of charge-carrier scattering in lead telluride. *Semiconductors*, 31(2), 173 – 176. <https://doi.org/10.1134/1.1187322> .

11. Knura R., Parashchuk T., Yoshiasa A., Wojciechowski K.T. (2021). Origins of low lattice thermal conductivity of $Pb_{1-x}Sn_xTe$ alloys for thermoelectric applications. *Dalt. Trans.*, 50 (12), 4323–4334. <https://doi.org/10.1039/d0dt04206d>.
12. Chesnokova D.B., Kamchatka M.I. (2001). Modeling of defect formation in lead chalcogenides and their properties. *Inorg. Mater.* 37(2), 111–118. <https://doi.org/10.1023/A:1004189006526>.
13. Sealy B.J., Crocker A.J. (1973). The P-T-x phase diagram of PbTe and PbSe. *Journal of Materials Science*, 8, 1737–1743.

Submitted: 07.05.2025

Горічок І.В.¹ (<https://orcid.org/0000-0001-9748-3288>),
Галушчак М.О.² (<https://orcid.org/0009-0000-3693-4903>),
Кулик О.Г.¹ (<https://orcid.org/0009-0001-2499-6813>)
Потятинник Т.С.¹ (<https://orcid.org/0009-0004-7067-7639>)

¹ Прикарпатський національний університет
імені Василя Стефаника, м. Івано-Франківськ, 76018, Україна;
² Івано-Франківський національний технічний університет нафти і газу,
м. Івано-Франківськ, 76000, Україна

Розрахунок рухливості носіїв заряду у PbTe на основі емпіричних термоелектричних параметрів

У роботі проведено порівняльний аналіз рухливості носіїв заряду у PbTe розрахованої з використанням виразів отриманих на основі моделі Друде-Зомерфельда та моделі невиродженого напівпровідника з параболічними зонами. При цьому рухливості розраховувались як функції експериментально визначених коефіцієнта Зеебека та питомої електропровідності. Результати співставлено з відповідними даними отриманими в наближенні часу релаксації.

Ключові слова: рухливість, коефіцієнт Зеебека, питома електропровідність, ефективна маса.

Надійшла до редакції 07.05.2025